The Astrophysical Journal, 802:80 (13pp), 2015 April 1 doi:10.1088/0004-637X/802/2/80

TITANIUM ISOTOPE SOURCE RELATIONS AND THE EXTENT OF MIXING IN THE PROTO-SOLAR NEBULA EXAMINED BY INDEPENDENT COMPONENT ANALYSIS

Robert C. J. Steele and Patrick Boehnke
Department of Earth, Planetary, and Space Sciences, University of California, Los Angeles, CA 90095, USA
Received 2014 July 24; accepted 2014 December 12; published 2015 March 25

ABSTRACT

The Ti isotope variations observed in hibonites represent some of the largest isotope anomalies observed in the solar system. Titanium isotope compositions have previously been reported for a wide variety of different early solar system materials, including calcium, aluminum rich inclusions (CAIs) and CM hibonite grains, some of the earliest materials to form in the solar system, and bulk meteorites which formed later. These data have the potential to allow mixing of material to be traced between many different regions of the early solar system. We have used independent component analysis to examine the mixing end-members required to produce the compositions observed in the different data sets. The independent component analysis yields results identical to a linear regression for the bulk meteorites. The components identified for hibonite suggest that most of the grains are consistent with binary mixing from one of three highly anomalous nucleosynthetic sources. Comparison of these end-members show that the sources which dominate the variation of compositions in the meteorite parent body forming regions was not present in the region in which the hibonites formed. This suggests that the source which dominates variation in Ti isotope anomalies between the bulk meteorites was not present when the hibonite grains were forming. One explanation is that the bulk meteorite source may not be a primary nucleosynthetic source but was created by mixing two or more of the hibonite sources. Alternatively, the hibonite sources may have been diluted during subsequent nebula processing and are not a dominant solar system signatures.

Key words: astrochemistry – meteorites, meteors, meteoroids – methods: statistical – nuclear reactions, nucleosynthesis, abundances – protoplanetary disks – supernovae: general

1. INTRODUCTION

Isotope anomalies in primitive meteorites and their components can be used to examine the nucleosynthetic origins of the solar system (e.g., Lee et al. 1978). The various materials we sample in meteorites, for example, calcium, aluminum rich inclusions (CAIs), chondrules, and achondrites, formed in different parts of the proto-solar nebula, and at different times. Therefore, these samples naturally record some of the variation in isotopic compositions present in the early solar system. Investigation of the differences in anomalies between these distinct materials can be used to examine their genetic relationships and the processes by which the different sources were mixed together to yield the variation in compositions we observe today.

Isotope anomalies in refractory elements with more than four isotopes, for example, Ti, Ni, and Mo, are highly correlated through the bulk meteorites, both chondrites and achondrites, and the population of normal CAIs (e.g., Trinquier et al. 2009; Steele et al. 2011, 2012; Burkhardt et al. 2011). This systematic variation occurs in most early solar system objects. There are, however, a few notable exceptions to this systematic variation, most interestingly the FUN (fractionated with unknown nuclear effects) CAIs and the CM hibonite grains. It is not clear how these populations of refractory inclusions, which are found in primitive meteorites, fit into the evolution of the wider solar system.

Hibonite, the focus of this study, is a highly refractory mineral thought to have been one of the first minerals to have formed in the solar system either as a refractory residue or by condensation from a nebula gas (Ireland et al. 1988). Hibonite grains from the CM carbonaceous chondrites (CCs) exhibit some of the largest isotope anomalies of any materials thought to have formed within the solar system. The evidence that the hibonite grains are of solar origin stems from their O isotope compositions within the normal range for solar system objects (Fahey et al. 1987a; Ireland et al. 1992; Liu et al. 2009). However, they exhibit ^{50}Ti enrichments of up to 27% (Ireland 1990) and deficits of up to 7% (Hinton et al. 1987). Several populations of hibonite grains have been documented in the literature (Ireland et al. 1988; Marhas et al. 2002), though they can broadly be split into two groups based on their petrology and their isotopic compositions. The first group is petrologically characterized by platy hibonite crystal fragments (PLACs from Ireland et al. 1988) and blue aggregates (BAGs from Ireland et al. 1988). This group shows the large mass-independent isotope anomalies in elements such as Ti and Ca described above and no evidence for live short-lived radionuclides (SLRs) such as ^{26}Al (Ireland et al. 1988; Ireland 1990). The second group, comprised of spinel and hibonite rich spherules (SHIBs from Ireland et al. 1988), show much smaller mass-independent isotope anomalies but do show evidence of live SLRs, for example, canonical or supra-canonical ^{26}Al (Ireland et al. 1988; Ireland 1990; Liu et al. 2009).

The large variation of mass-independent isotope anomalies found in hibonites is thought to represent either pure, or only slightly diluted, presolar signatures (e.g., Ireland 1990). However, it is not known if the events that produced the hibonites occurred within the solar system at some time before the large-scale chemical and isotopic homogenization. Alternatively, the hibonites may have formed outside the solar system, possibly closer to the source of the isotopic anomalies, for example, around a star in some region of the molecular cloud that had similar oxygen isotope compositions. Therefore, it is clearly of great importance to assess the relationship of the anomalies observed in the hibonites to those observed in bulk meteorites and other solar system materials. Examining these relationships will offer insight into whether the hibonites represent purer samples of the isotopic precursors of the bulk solar system,

sampled by the bulk meteorites, or if they represent a previously unsampled reservoir. An example of this type of finding is the recent discovery of oxide grains highly enriched in ^{54}Cr, which are thought to be the carrier phase of mass-independent Cr isotope anomalies in the solar system (Dauphas et al. 2010; Qin et al. 2011). The alternative, that the hibonites formed outside the solar system, possibly prior to solar system formation, would mean that hibonite grains do not have isotopic significance for the bulk solar system. Rather they represent a new population of presolar grain that is physically an order of magnitude larger than the previous largest population (with the exception of certain very rare examples; e.g., Zinner et al. 2010). However, previous presolar grain populations have very large O isotope variations, several orders of magnitude larger than those observed in CM hibonites (Fahey et al. 1987b; Zinner 2003).

In order to examine the relationships between hibonite grains and bulk meteorites common data must be examined to find similarities. With the exception of O, Ti is the element that has been most extensively studied in a wide variety of early solar system materials, including hibonite grains, FUN, and normal CAIs and bulk meteorites. Though O has been more extensively studied, it is not suitable for this purpose for two reasons. First, the origins of O isotope variations are debated and may have non-unique sources (Thiemens 1999; Lyons & Young 2005; Lyons et al. 2009). Moreover, there has clearly been subsequent mixing between these different solar system reservoirs. Second, O only has three isotopes, so only one mass-independent ratio, which limits the scope for analyzing sources. For these reasons we focus on Ti.

The first studies of Ti were in the FUN CAIs by the ANU and Caltech groups (Heydegger et al. 1979; Niemeyer & Lugmair 1980). These rare inclusions exhibited large anomalies in Ti, ± 40 $^{0}/_{000}$ on ^{50}Ti, where $^{0}/_{000}$ is the ε unit defined as the parts per ten thousand difference to a terrestrial standard. Several other elements show similar variation, for example, 150 $^{0}/_{000}$ on ^{48}Ca (Lee et al. 1978) and 290 $^{0}/_{000}$ on ^{58}Fe (Völkening & Papanastassiou 1989). Interestingly, these large anomalies on ^{58}Fe are unique in the solar system as no other objects have been found to show iron isotopic variation (e.g., Dauphas et al. 2008). Even larger anomalies were found in the hibonite grains from CM chondrites (e.g., Fahey et al. 1985; see above). Smaller, but still significant, Ti isotope anomalies were subsequently observed in the normal population of CAIs (e.g., Niemeyer & Lugmair 1981) and in bulk meteorites (e.g., Leya et al. 2008).

In general, the early studies of Ti isotopes in chondritic inclusions and hibonites grains showed large anomalies on the neutron rich isotope ^{50}Ti and smaller anomalies on the other isotopes. However, no coherent correlations have been observed in the Ti isotope compositions from these samples. These studies were focused on examining the input of neutron-rich isotopes to the early solar system, principally because of the early identification of anomalies on ^{48}Ca in FUN CAIs (Lee et al. 1978), which led to the almost universal use of normalization to ^{46}Ti/^{48}Ti for the mass-dependent fraction correction in early studies. Fahey et al. (1987a) examined the number of sources required to produce the variation in Ti isotope compositions by fitting the data to a plane with a least squares algorithm similar to the more conventional York regression for two-dimensional correlation. Fahey et al. (1987a) concluded that at least four, possibly more, sources were needed to reproduce the observed compositions.

In contrast, the more recent, high precision data for bulk meteorites show a striking correlation between $\varepsilon^{50}\mathrm{Ti}_{(47/49)}$ and $\varepsilon^{46}\mathrm{Ti}_{(47/49)}$, where the subscripts denote the normalizing ratio; see Section 2.1 (Leya et al. 2008, 2009; Trinquier et al. 2009; Zhang et al. 2011, 2012). This correlation was shown by Qin et al. (2011) and Steele et al. (2012) to be consistent with input from the O/Ne zone of a type II supernova (SN II). Mass-independent isotopic variation between different bulk meteorite groups likely represents much more anomalous Ti by mass than the much larger anomalies seen in the hibonite grains.

One obvious hypothesis for the origin of Ti isotope variation in the solar system is that one of the sources present in the hibonite grains is also the source represented by the variation observed in the bulk meteorites. Relationships between hibonites and other meteorite groups were investigated by previous studies, for example, Fahey et al. (1987a). Since these early investigations, more higher-quality data have been reported, especially in the bulk meteorite populations; therefore, this subject is worth revisiting. The aim of this paper is to test the hypothesis that one of the sources present in the compositions of the hibonites and FUN CAIs is the same source observed in the bulk meteorites. This will enable us to examine the reasons why multiple sources are observed in the meteoritic inclusions (hibonites and FUN CAIs) while only one appears to be sampled by the bulk meteorites.

2. METHODS

2.1. Renormalization

Mass-independent isotope anomalies require normalization for mass-dependent fractionation. This is normally achieved using one isotope ratio to calculate and remove the expected fractionation on the other ratios, a process termed "internally normalizing." See Russell et al. (1978), McCulloch & Wasserburg (1978), and Young et al. (2002) for discussions of fractionation corrections and the choice of fractionation "laws." Many of the hibonite data were original presented normalized to ^{46}Ti/^{48}Ti by the exponential law. These data have been renormalized to ^{47}Ti/^{49}Ti to make them comparable with the more recent bulk data for which $\varepsilon^{50}\mathrm{Ti}_{(47/49)}$ and $\varepsilon^{46}\mathrm{Ti}_{(47/49)}$ anomalies have been observed. It is important for the independent component analysis (ICA; see below) that appropriate uncertainties propagated through the normalization. To ensure renormalized uncertainties are appropriate, they have been modeled using a Monte Carlo simulation by varying the data around their original uncertainties and propagating this through the full renormalization. This was repeated 10,000 times to fully map the parameter space, and the renormalized uncertainty is then the standard deviation (s.d.) of these repeats. The code used for the renormalization was written using R (R Core Team 2013) and is available on request. The renormalized data are given in Table A1 and are plotted in Figure 1.

2.2. Independent Component Analysis

ICA is a method of blind source separation by which a multivariate data set can be deconvolved into independent subcomponents (Comon 1994). That is, a data set, in this case Ti isotope data from hibonites, can be examined for the sources that mixed to produce the observed variation. ICA is related to the more commonly used principal component analysis but differs in that the components identified do not have to be orthogonal. ICA relies on two assumptions; first, that the sources are statistically independent from each other, and second, that mixing between sources is linear. ICA algorithms work by finding solutions that

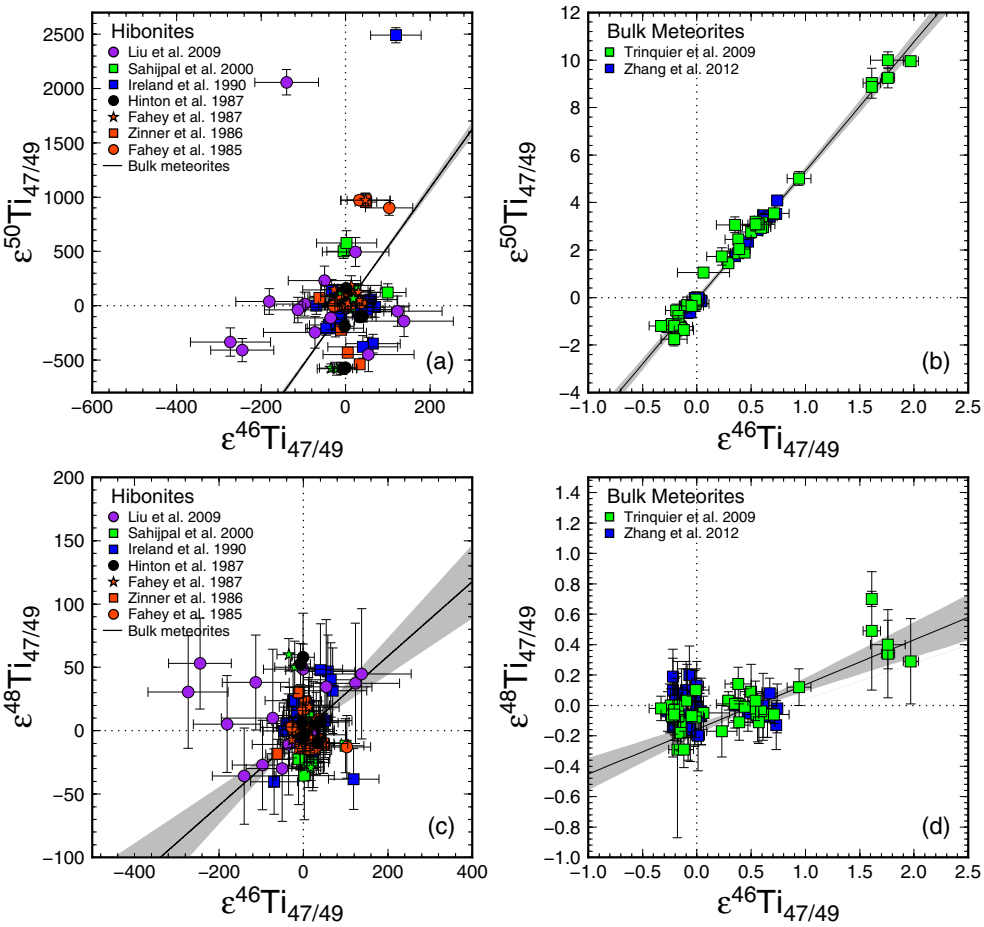

Figure 1. Figures showing previous Ti isotope compositions for hibonites (a) and (c) (from Fahey et al. 1985; Zinner et al. 1986; Fahey et al. 1987a; Hinton et al. 1987; Ireland 1990; Sahijpal et al. 2000; Liu et al. 2009), bulk meteorites and normal CAIs (b) and (d) (from Trinquier et al. 2009; Zhang et al. 2011, 2012). Also shown on both pairs of plots are extrapolations, with error envelopes, of the slopes from bulk meteorites and normal CAIs determined by York Regression (York 1969; Mahon 1996).

minimize the shared information between components and maximizing the non-Gaussianity of the individual components. The ICA algorithm returns a component, or vector, along which a significant proportion of the variation observed in the data set as a whole can be described. Where significant variation remains, more components can be added until the data set can be fully described. The components describe a slope that is a mixing line to a composition that represents one of the sources required to produce the variation in the data. These vectors, or components, may share a source at one end, or all sources may be independent, so there must be at least n+1 sources where n is the number of components. Therefore, three vectors may represent between four and six isotopic source compositions. To describe the vector, the ICA reports a point and the vector is the slope to the origin in n dimensions. These points may be in either positive or negative fields because the ICA only determines the vector and the sign is assigned randomly. For a full description of ICA, see Hyvärinen and Oja (2000).

There have been two previous studies in geochemistry and cosmochemistry that have used ICA for investigating source relationships. These looked at the distribution of mantle sources from the isotopic compositions of MORBs and OIBs (Iwamori & Albarède 2008) and the mixing relations in the HED suite of meteorites by examining major element abundances (Usui & Iwamori 2013). As they discuss, it is not clear that the requirement for straight line mixing is satisfied in the study of Iwamori & Albarède (2008) as in some cases they include isotope data from several different elements. Where different elements are used, mixing will only approximate straight line mixing if the denominator isotopes are of the same concentration. It is important to note that in this study mixing is linear in Ti isotope space as all the ratios use the same denominator isotope.

We have used the FastICA algorithm of Hyvarinen (1999); Hyvärinen and Oja (2000) implemented in an R (R Core Team 2013) script by Marchini et al. (2013) to determine the independent components of Ti isotope data. A limitation of the traditional ICA is that uncertainties are not taken into account. This is because for the situations in which ICA has normally been applied, the majority of the noise in the data set does not come from measurement uncertainties, rather from real variation in the data.

We have extended the traditional ICA by combining it with a Monte Carlo simulation of the uncertainties, or bootstrap (Efron 1981), of the data in order to gain a statistical measure of the uncertainty of the independent components determined by the FastICA algorithm. The isotopic data were varied randomly around their averages with a Gaussian distribution and an ICA performed for each iteration; this was repeated 20,000 times to achieve a robust measure of the uncertainty. We have used clustering algorithms to sort the data into the individual components (Fritz et al. 2012; Cuesta-Albertos et al. 1997). During this process, 1% of the models were discarded (e.g., tclust $\alpha = 0.01$) because they did not fit into any of the clusters. This loss of data is taken into account in the eventual uncertainty.

The clustering algorithms were optimized to use equal weights to ensure that the clusters contained equal numbers of points. The R scripts used to perform the ICA are available on request.

The results of these iterations produce a number of vectors that describe a mixing line toward the source and are illustrated by the distribution of points in Figure 2. The vectors form clusters, the number of which is twice the number of components used because the vector may be either positive or negative from the origin; each pair of clusters describes the distribution of one component. The variation within a cluster of vectors describes the uncertainty in the component and includes contributions from the analytical uncertainty of the data and the uncertainty inherent in the ICA algorithm. This gives a robust measure of the uncertainty of the components determined by the ICA and allows components from different sample populations to be compared.

2.3. Data Used in the ICA

We have performed the ICA on both the hibonite and bulk meteorite data sets. We have used hibonite data for SHIBs, PLACs, and BAGs from as many studies possible, including measurements from Fahey et al. (1985), Zinner et al. (1986), Fahey et al. (1987a), Hinton et al. (1987), Ireland (1990), Sahijpal et al. (2000), and Liu et al. (2009). The data from these studies were collected over 25 yr on a variety of ion probes; however, they all provide measurements from the standard Madagascar hibonite that are in agreement warranting their inclusion in this metadata set.

Several recent studies have measured the Ti isotope compositions of bulk meteorites and normal CAIs (Leya et al. 2008, 2009; Trinquier et al. 2009; Zhang et al. 2011, 2012). However, not all of these studies are appropriate to include in a metadata set. The recent Ti studies of bulk meteorites and normal CAIs all show broadly consistent results finding correlated anomalies on $\varepsilon^{50}\mathrm{Ti}_{(47/49)}$ and $\varepsilon^{46}\mathrm{Ti}_{(47/49)}$, with very little variation on $\varepsilon^{48}\mathrm{Ti}_{(47/49)}$. Trinquier et al. (2009) and Zhang et al. (2011, 2012) report very high precision Ti isotope compositions for a wide range of bulk meteorites, both chondrites and achondrites. In addition, Trinquier et al. (2009) report Ti isotope compositions for the normal population of CAIs. Though the earlier studies of Leya et al. (2008, 2009) show broadly similar results to the more recent studies, they are of lower precision and so would hamper our ability to determine the slopes of mixing. Leya et al. (2008) also raise concerns over large non-terrestrial blanks introduced to some of their samples during digestion in Teflon bombs that may have affected the accuracy of some data. Therefore, we do not include the results of Leya et al. (2008, 2009) in our metadata set. Correlations produced by the studies of Trinquier et al. (2009) and Zhang et al. (2011, 2012) are very consistent. In $\varepsilon^{46}\mathrm{Ti}_{(47/49)}$versus $\varepsilon^{50}\mathrm{Ti}_{(47/49)}$, they produce slopes of 5.48 ± 0.27 and 5.23 ± 0.22 for Trinquier et al. (2009) and Zhang et al. (2011, 2012), respectively. A "new" York regression (Mahon 1996) based on this combined data set yields 5.37 ± 0.15.

2.4. ICA Data Presentation and Mixing Angles

In order to compare the sources of different sample populations, the mixing vectors of each cluster, and the variation in these vectors within each cluster, must be compared. The data are presented initially by simply plotting the points returned by the ICA. In order for the components obtained from different sample populations to be compared on the same diagram, the data for each point, in each individual dimension, has been normalized to the sum of the standard deviations of each dimension. This was achieved using

$$\gamma\left({}^{j}Ti_{\frac{47}{49}}\right) = \frac{i\left({}^{j}Ti_{\frac{47}{49}}\right)}{\sigma\left({}^{j}Ti_{\frac{47}{49}}\right) + \sigma\left({}^{k}Ti_{\frac{47}{49}}\right) + \sigma\left({}^{l}Ti_{\frac{47}{49}}\right)}, \quad (1)$$

where $\gamma({}^{j}\mathrm{Ti}_{(47/49)})$ is the renormalized component composition for the ith iteration of the ICA in the dimension of $({}^{j}\mathrm{Ti}_{(47/49)})$ (where isotope ${}^{j}\mathrm{Ti}$ which was normalized for mass-dependent fractionation using the ${}^{47}\mathrm{Ti}/{}^{49}\mathrm{Ti}$ ratio); j, k, and l represent the isotopes of Ti; $i({}^{j}\mathrm{Ti}_{(47/49)})$ is the raw composition of the ith iteration of the ICA in the dimension of $({}^{j}\mathrm{Ti}_{(47/49)})$ and $\sigma({}^{j}\mathrm{Ti}_{(47/49)})$; $\sigma({}^{k}\mathrm{Ti}_{(47/49)})$ and $\sigma({}^{l}\mathrm{Ti}_{(47/49)})$ are the standard deviations over all iterations of the ICA in the dimensions of $({}^{j}\mathrm{Ti}_{(47/49)})$, $({}^{k}\mathrm{Ti}_{(47/49)})$, and $({}^{l}\mathrm{Ti}_{(47/49)})$, respectively. Thus, the total variation of each sample population can be presented in the same, albeit artificial, range. Importantly though, the angular information is retained, so the slopes, or angles, of the components hold through this normalization.

In order to quantitatively compare the components obtained for different sample populations, the vectors must be obtained from the slopes. Previous studies have used the approach of comparing slopes of mixing in order to compare data sets (e.g., Dauphas et al. 2004; Steele et al. 2012). In these previous cases, the data sets being compared were bulk meteorite data and modeled nucleosynthetic data for different astrophysical environments, not different populations of measurements, but the concepts are the same. The use of slopes has some associated problems for comparison of different data sets. The major problem with slopes is that when they approach the vertical or horizontal the slope loses linearity and tends to zero or infinity. This reduces the ability to graphically resolve the difference between multiple slopes of different magnitudes. More seriously, however, if the uncertainty of a slope crosses the vertical axis, it will artificially encompass both zero and infinity making statistical comparison between different uncertainties more complicated.

The issue of infinities may be simplified by using the angles of mixing (where $\theta = \arctan(m)$ ensuring the result is in degrees) rather than slopes of mixing (m). Angles of mixing have the advantage that they are linear and contain only one singularity (360 to 0, where 0 is the positive limb of the x axis) compared to the four of slopes. This means that for comparison of two mixing lines (and possibly more) a position of the singularity may be chosen so that none of the uncertainties are affected. In this study mixing lines are presented as angles of mixing and not slopes. This method could be useful in other areas, for example, the comparison of mixing of nucleosynthetic environments in to the solar system.

3. RESULTS OF THE ICA

The results of the ICA are presented in Table 1 and Figures 2(a), (b), (c), (d), and 3.

3.1. ICA Components

Figures 2(a), (b), and (c) show the ICA components presented as $\gamma({}^{j}\mathrm{Ti}_{(47/49)})$ normalized data showing the hibonite and bulk meteorite data.

As expected, the results of the ICA for the bulk meteorite data, shown in red in Figure 2(a), show a very clear correlation

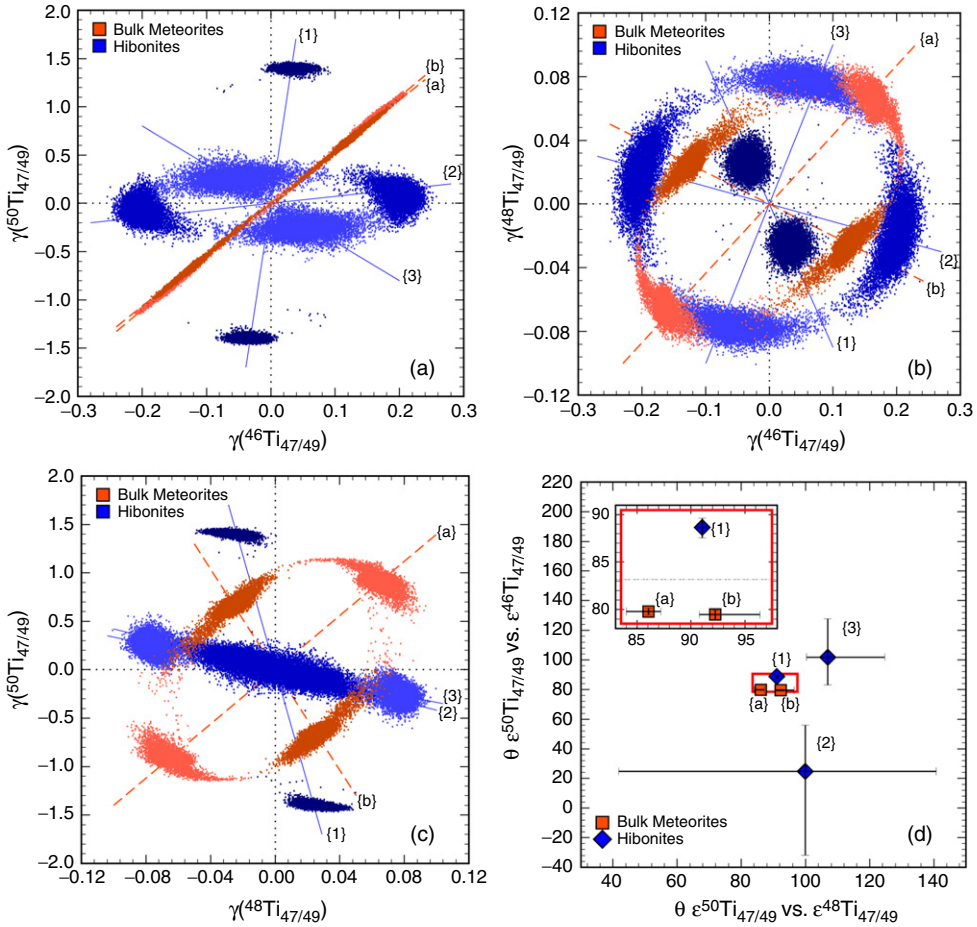

Figure 2. Figures showing the results of the ICA bootstrap for both the hibonite and bulk meteorite data. Plots (a), (b), and (c) show all the raw compositions of the ICA bootstrap iterations with the exception, in the case of the hibonites, of 1% of components that are so far away from an average component composition that they cannot be grouped. The individual components are highlighted by different shades and labeled with {1}, {2}, {3}, {a}, and {b}. Plot (d) shows the slopes of mixing of the different components and their uncertainties. By plotting $\theta\ \varepsilon^{50}\mathrm{Ti}_{(47/49)}$ vs. $\varepsilon^{46}\mathrm{Ti}_{(47/49)}$ against $\theta\ \varepsilon^{50}\mathrm{Ti}_{(47/49)}$ vs. $\varepsilon^{48}\mathrm{Ti}_{(47/49)}$, we use all Ti isotope dimensions. These plots show that the dominant sources present in the bulk meteorite data are not represented in the hibonite data as all hibonite components are resolved from both bulk meteorite components in both dimensions. (The only exception is the hibonite component {3} in $\theta\ \varepsilon^{50}\mathrm{Ti}_{(47/49)}$ vs. $\varepsilon^{48}\mathrm{Ti}_{(47/49)}$, which is very poorly defined and has essentially 100% uncertainties.) The errors are the 95% confidence intervals from the distribution of the bootstrapped ICA components. The dashed line in the inset figure is the lower error bound of hibonite component {3}.

Table 1
Results of the ICA on the Hibonite and Bulk Meteorite Populations

	Average	−2 s.d.	+2 s.d.
	$\varepsilon^{50}\mathrm{Ti}_{(47/49)}$ vs. $\varepsilon^{46}\mathrm{Ti}_{(47/49)}$		
Bulk {a}	79.784	0.323	0.347
Bulk {b}	79.467	0.519	0.442
Hibonite {1}	88.673	1.126	0.962
Hibonite {2}	24.342	56.666	31.094
Hibonite {3}	101.968	18.662	26.189
	$\varepsilon^{50}\mathrm{Ti}_{(47/49)}$ vs. $\varepsilon^{48}\mathrm{Ti}_{(47/49)}$		
Bulk {a}	86.069	2.059	1.146
Bulk {b}	92.264	1.492	4.145
Hibonite {1}	91.040	0.459	0.463
Hibonite {2}	100.075	60.164	43.414
Hibonite {3}	106.891	6.463	18.400

Notes. The results are presented as the angle ($\theta^\circ = \arctan(m)$ ensuring the result is in degrees, where m is the slope) of mixing vectors to the returned components. The uncertainties are 95% confidence intervals derived from the spread of the ICA components returned by the bootstrap. Note the errors are the deviation in angle and are not symmetrical.

between $\gamma(^{50}\mathrm{Ti}_{(47/49)})$ and $\gamma(^{46}\mathrm{Ti}_{(47/49)})$. In Figures 2(b) and (c), which include the other dimension $\gamma(^{48}\mathrm{Ti}_{(47/49)})$, the components are not correlated. The divergence from a single correlation, and the presence of well defined components, shows that variation in $\varepsilon^{48}\mathrm{Ti}_{(47/49)}$ is observed and the mixing vectors of the sources can be examined by the ICA.

3.2. ICA Angles

The single, tight correlation observed between $\varepsilon^{46}\mathrm{Ti}_{(47/49)}$ and $\varepsilon^{50}\mathrm{Ti}_{(47/49)}$ in the bulk meteorites can be used as a test of the accuracy of the ICA method for determining the mixing slopes of the sources and also the uncertainty estimation by our bootstrap method (see Figure 3). Regardless of any variation in $\varepsilon^{48}\mathrm{Ti}_{(47/49)}$, a projection of the plane present in the bulk meteorites on to the $\varepsilon^{50}\mathrm{Ti}_{(47/49)}$ versus $\varepsilon^{46}\mathrm{Ti}_{(47/49)}$ axis will be a single correlation. This holds for line fitting algorithms, such as the least squares York regression and ICA. Therefore, the slopes and errors obtained by York regression and ICA can be compared. This offers a demonstration of the accuracy of the angle obtained by the ICA and the precision of this method relative to the uncertainty of the original data. A "new" York regression on the combined data set of Trinquier et al. (2009) and Zhang et al.

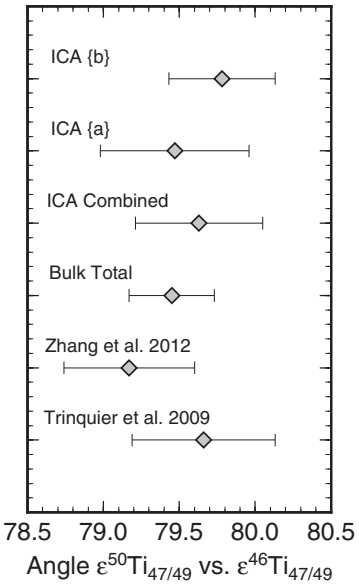

Figure 3. Figure showing a comparison between the estimates of angle of the bulk meteorite Ti isotope data in $\varepsilon^{50}\mathrm{Ti}_{(47/49)}$ vs. $\varepsilon^{46}\mathrm{Ti}_{(47/49)}$ estimated by York regression and ICA. The results of the two estimations are very similar, which displays the power of ICA to estimate the slopes of correlations within data. ICA{a} and ICA{b} are the two components that are determined for the bulk meteorite population.

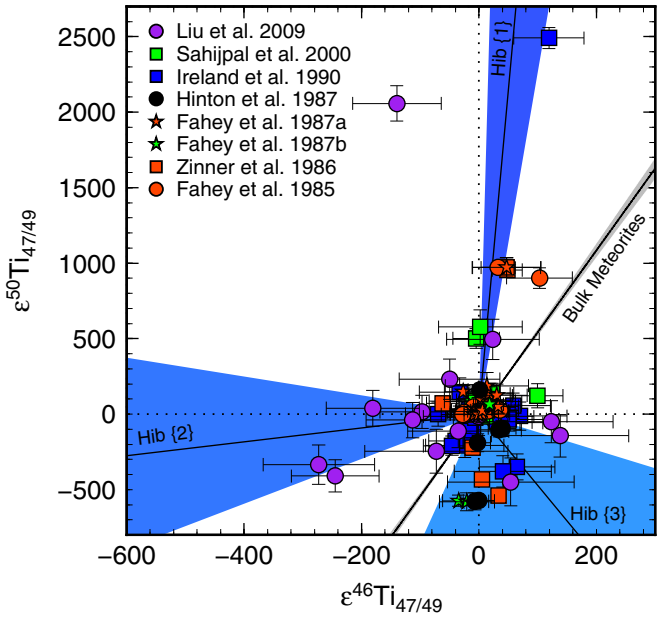

Figure 4. Figure showing the Ti isotope compositions for hibonite grains and the components determined from the ICA. The data, with only a few exceptions, are within error of one of the components. This suggests that there is no requirement for a further components. The compositions of few points that lie outside of error of all the components can be created by mixing two of the components.

(2012) yields a slope of 5.37 ± 0.15, the angle obtained from this slope is $79.45 \pm 0.29^{\circ}$. This value is very close to the average value obtained by the ICA of $79.63 \pm 0.42^{\circ}$ (see Figure 3). Moreover, the uncertainties are also very similar, with the uncertainty slightly larger as expected as it includes a potential contribution from the ICA algorithm. This displays the ability of ICA to return accurate and precise vectors of source mixing.

4. DISCUSSION

The results of the ICA show clear differences between character of the sources represented in the hibonite population versus the bulk meteorites and the normal CAIs (see Figure 2). The most obvious explanation for this would be that the sources represented by the hibonite and bulk meteorites populations are different. The implications of this explanation are discussed in detail in Section 4.3. However, there are several other possible reasons why the components represented by these two populations might be different. First, the sources represented by the bulk meteorites and normal CAIs might be mixtures of the hibonite sources. Second, the hibonite population may represent more sources than the four to six that can be examined by a three dimensional ICA. Last, there could be a combination of these possibilities and the three hibonite components represent more than six sources and that the bulk meteorite compositions are mixtures between some of these sources. The likelihood and implications of these more complex scenarios are discussed below.

4.1. Number of Sources

The simplest explanation of the isotopic variation observed by the ICA is that the hibonites represent between four and six sources and the bulk meteorites and normal CAIs represent between three and four. These are the simplest explanations because they represent the fewest number of anomalous sources in the solar system that can entirely explain the variation we observe. However, more complex models that involve more sources or mixing of sources are possible.

4.1.1. Number of Sources Represented by the Hibonites

The hibonite system is underconstrained in that there are at least as many required components as dimensions. It is very difficult to examine how many components are required by an underconstrained system and impossible to conclusively test. However, there are certain arguments and lines of evidence that suggest that the hibonite data, at the current level of precision, are only showing evidence for three components. First, four sources can describe any three-dimensional data array; akin to a point lying on a mixing line between two sources, there is no mathematical requirement for more sources to explain the spread of the data. Second, the components we have identified closely resemble the data with the largest variation in $\gamma(^{50}\mathrm{Ti}_{(47/49)})$, followed by $\gamma(^{46}\mathrm{Ti}_{(47/49)})$, then $\gamma(^{48}\mathrm{Ti}_{(47/49)})$. Moreover, the angles of these components fit with the angles of the original data such that the errors of all but a few data overlap with the mixing vectors of the components (see Figure 4 and further discussion in Section 4.2.2). This demonstrates that the components are fully explaining the data without simply describing a cube around them. The most striking feature is that most data only require input from one component. Most hibonite data show evidence of binary mixing from one of three highly anomalous sources. Third, the ICA tries to explain the variation in a data set by making the sources as statistically independent as possible. Therefore, we can examine the possibility of unrepresented components by looking at the distribution of the three components we can identify.

As shown in Figure 2, the vector of component {1} is very different from the other two, this makes it very statistically resolved as this is a function of the angular separation and the distribution of point along the component vector. The angles of components {2} and {3} are much more similar. As the ICA hierarchically tries to assign components based on statistical

significance, a fourth, unresolved component must be at least as similar to one of the other components as {2} and {3} are to each other or else it would have been chosen. If a fourth component were to be present and unrepresented, it would most likely lie in the plane of the {2} and {3} components as this is where several of the data that are not within error of a component vector reside. It is possible that if such a component exists it could be represented by the SHIB hibonite population, which are currently largely within error of terrestrial values.

A higher precision Ti isotope study of hibonite would significantly help resolve issues surrounding the number of sources. However, as the data stand with the PLAC population essentially showing all the variation, for the reasons described above, the most likely explanation is three components and four sources. We discuss the compositions of these sources in more detail below (see Section 4.2).

4.1.2. Number of Sources Represented by the Bulk Meteorites

The variation observed in the bulk meteorites is well described by two components, or at least three sources. This finding is in agreement with previous studies that show that there must be more than two sources in the bulk meteorite and normal CAI system (Trinquier et al. 2009; Williams et al. 2014). There is a hint in the bulk meteorite and normal CAI data that the third anomalous source is only present in the CAIs. This is because a York regression on the bulk meteorite population, without the normal CAI data, yields a slope of zero in $\varepsilon^{50}\mathrm{Ti}_{(47/49)}$ versus $\varepsilon^{48}\mathrm{Ti}_{(47/49)}$. Moreover, an ICA on the bulk meteorites alone shows no variation in the $\gamma(^{48}\mathrm{Ti}_{(47/49)})$ dimension. This is supported by Williams et al. (2014), who have reported evidence for a third source in chondrules and CAIs in the absolute Ti isotope compositions. Absolute ratios include both natural mass-dependent fractionation and mass-independent anomalies, thus showing the true location and magnitude of the anomalies. Absolute ratios have previously been reported for Ti in CAIs (Niederer et al. 1985) and Ni in bulk meteorites (Steele et al. 2012). Interestingly, Trinquier et al. (2009) found evidence for a third source in leachates from CI CC, which depart from the single correlation of the bulk meteorites. However, the carrier phase of this variation is likely much more homogeneously distributed between different chondrite parent bodies and so is not observed in bulk dissolutions of meteorites as has been observed for other elements (e.g., Schönbächler et al. 2005; Trinquier et al. 2008). The variation from the leachates, however, does superficially look more like the variation seen in the hibonites, with significantly more variation in $\varepsilon^{50}\mathrm{Ti}_{(47/49)}$ creating a near vertical trend (see Figure 3 of Trinquier et al. 2009).

4.1.3. Bulk Meteorites as Mixtures of Hibonite Sources

One further possibility is that the components observed in the bulk meteorites and normal CAIs are mixtures of the sources represented by the hibonites. It is important to note that the bulk meteorite population is overdescribed as it is fully described by fewer components than dimensions. The maximum number of sources is four and the most likely is three. The three most likely sources are an average, old molecular cloud composition and two anomalous sources. The identities of the sources are discussed in more detail in Section 4.2. The two anomalous sources could both be hibonite sources or one could be an independent presolar carrier phase. This scenario is possibly somewhat less likely because it requires an extra stage of discrete mixing between the formation of hibonites and the formation of the normal CAIs and bulk meteorites.

4.2. Source Compositions

First, it is important to note that the ICA returns a vector along which the source composition lies. Therefore, it is not possible to say exactly what the source composition is, just the angle of its mixing line. However, by using the angles of the mixing lines we can identify compatible nucleosynthetic sources in the same way that York regressions on data have been used to examine nucleosynthetic sources in the past (e.g., Dauphas et al. 2004; Steele et al. 2012).

4.2.1. Source Compositions of Bulk Meteorite Components

The two components that the bulk meteorites and normal CAIs require are identical within error in $\gamma(^{50}\mathrm{Ti}_{(47/49)})$ versus $\gamma(^{46}\mathrm{Ti}_{(47/49)})$ and have angles identical to a York regression in the same dimensions on the original data of Trinquier et al. (2009; see Figure 2). This suggests binary mixing in $\varepsilon^{46}\mathrm{Ti}_{(47/49)}$ and $\varepsilon^{50}\mathrm{Ti}_{(47/49)}$ to produce this line. This source has been previously suggested to be input from the O/Ne zone of an SN II (Qin et al. 2011; Steele et al. 2012). The compositions produced by the O/Ne zones of SN II vary with the mass of the pre-supernova star. Few of the models of Rauscher et al. (2002) match exactly the slopes required to explain Ti isotope variation in the solar system; they are however, all close. Titanium-50 and ^{46}Ti are thought to be dominantly produced in different nucleosynthetic environments. Therefore, the finding that by including anomalies on the normalizing isotopes the correct slopes of mixing may be produced is itself important. An alternative hypothesis to explain the meteorite correlation is simultaneous mixing of two distinct nucleosynthetic sources, one with $\varepsilon^{46}\mathrm{Ti}_{(47/49)}$ anomalies and one with $\varepsilon^{50}\mathrm{Ti}_{(47/49)}$ anomalies, within the solar system due to some common process (Trinquier et al. 2009). The ICA analysis is consistent with either interpretation.

In the other Ti axis, $\gamma(^{48}\mathrm{Ti}_{(47/49)})$, however, there is a slight variation between the two components. Note that the scale of the $\gamma(^{48}\mathrm{Ti}_{(47/49)})$ axis in Figure 2(c) significantly magnifies the apparent difference and the two components are in fact only divergent by 6°. Component {a} shows a positive correlation with an angle of $86.1^{+1.2}_{-2.1}$°, while component {b} is, in fact, almost vertical, so showing almost no influence on ^{48}Ti, with an angle of $92.3^{+4.7}_{-1.5}$°. The positive correlation in component {a} is just visible in the original meteorite and normal CAI data (see Figure 1(d)). However, the apparent correlation is only present in the CAI data. This may suggest that the CAIs are sampling a source that imparts a very slight anomaly in $\varepsilon^{48}\mathrm{Ti}_{(47/49)}$ and is not present in the bulk meteorite population. This inference may be supported by recent absolute Ti isotope measurements of Williams et al. (2014), who found evidence for correlated ^{46}Ti, ^{47}Ti, and ^{50}Ti anomalies in the bulk meteorites while the CAIs plotted off this trend in ^{47}Ti. It is not clear if this can explain the deviation in $\varepsilon^{48}\mathrm{Ti}_{(47/49)}$ observed in the previous measurements, but is supporting evidence that the CAIs may be sampling a subtly different set of sources. An ICA performed on the bulk meteorites alone yields one component identical in angle in $\gamma(^{50}\mathrm{Ti}_{(47/49)})$ versus $\gamma(^{46}\mathrm{Ti}_{(47/49)})$ to the two component ICA and with zero variation in $\gamma(^{48}\mathrm{Ti}_{(47/49)})$, which may support this hypothesis further. The major conclusions of this study are not affected by this debate because the variation in $\gamma(^{50}\mathrm{Ti}_{(47/49)})$ versus $\gamma(^{46}\mathrm{Ti}_{(47/49)})$ is not affected and the

variation in $\gamma(^{48}\mathrm{Ti}_{(47/49)})$ is very small and always resolved from the hibonite components. However, the hint that the CAIs, while dominated by the same anomalous sources as the bulk meteorites, may sample an additional anomalous source is very interesting. This finding could have significant implications for early solar system mixing and warrants further study.

4.2.2. Source Compositions of the Hibonite Components

The nucleosynthetic origins of the hibonite sources have been less well studied in a quantitative sense and the overall lack of precision in the components we have identified does not makes this endeavor much easier. Interestingly, the errors of most of the hibonite grains overlap with at least one of the identified components, for example, in $\varepsilon^{50}\mathrm{Ti}_{(47/49)}$ versus $\varepsilon^{46}\mathrm{Ti}_{(47/49)}$ (see Figure 4). This suggests the hibonite grains may mostly be exhibiting binary mixing to one anomalous nucleosynthetic source. In the rare cases of the remaining data that lie a long way from any of the component vectors, these compositions may be produced by mixing two of the anomalous nucleosynthetic sources. Mixing two sources is not an unexpected result as the ICA is designed to deconvolve multivariate data. Even so, a finding of binary mixing in the majority of the hibonites presents a simplified case that may offer more easily testable predictions for mixing in other isotope systems.

As discussed above, the components of the hibonites are not equally well defined. The most precisely defined component is component {1} with an angle of $88.7^{+1.0}_{-1.1}{}^{\circ}$ in $\gamma(^{50}\mathrm{Ti}_{(47/49)})$ versus $\gamma(^{46}\mathrm{Ti}_{(47/49)})$ and $91.0^{+0.5}_{-0.5}{}^{\circ}$ in $\gamma(^{50}\mathrm{Ti}_{(47/49)})$ versus $\gamma(^{48}\mathrm{Ti}_{(47/49)})$. These angles may be well defined enough to examine the nucleosynthetic significance, however, it is not clear where these signatures may be produced.

As with previous studies (e.g., Steele et al. 2012) we are looking for a signature that describes the characteristic of a distinct nucleosynthetic environment. The most significant finding is a feature that is consistent among most, if not all, models. For example, the ^{58}Ni anomaly found in the Si/S zone of all masses of SN II (Steele et al. 2012). We have compared the slopes of the hibonite components to the same range of supernova models as previous studies: for type Ia supernova (SN Ia), Woosley (1997), Travaglio et al. (2004), Iwamoto et al. (1999), Hashimoto (1995), Maeda et al. (2010), and Travaglio et al. (2011); for SN II, Iwamoto et al. (1999), Umeda & Nomoto (2002), Nomoto et al. (1997), Rauscher et al. (2002), and Hashimoto (1995); for asymptotic giant branch (AGB) stars, models were kindly provided by R. Gallino & A. Davis (2009, private communication); and for individual shells of SN II, we used models from Meyer et al. (1995) and Rauscher et al. (2002). Bulk homogenous SN II are not a likely candidate, both because it is unrealistic they would present a single homogenized signature, and also this signature does not produce the high $\varepsilon^{50}\mathrm{Ti}_{(47/49)}$ anomalies required. Large ^{50}Ti excesses are produced in the inner regions of SN II suggesting this as a possible candidate. However, these excesses are accompanied with significant deficits in ^{47}Ti, which in the $^{47}\mathrm{Ti}/^{49}\mathrm{Ti}$ normalization acts to reduce the apparent ^{50}Ti anomaly and increase the apparent ^{46}Ti anomaly, such that the slope in $\varepsilon^{50}\mathrm{Ti}_{(47/49)}$ versus $\varepsilon^{46}\mathrm{Ti}_{(47/49)}$ is always too low. Finally, large excesses in ^{50}Ti, not accompanied by excesses of ^{47}Ti or ^{46}Ti, are a general, if not universal, feature of SN Ia. This suggestion is further supported by the large positive ^{48}Ca anomalies, which are correlated with ^{50}Ti anomalies (e.g., Zinner et al. 1986). Large ^{48}Ca anomalies, in the absence of ^{46}Ca anomalies, are strong evidence for input from an SN Ia (Meyer et al. 1996). This makes SN Ia the most likely source for the high ^{50}Ti component in the hibonites, but is by no means conclusive.

The other two components are not nearly as well defined, and no nucleosynthetic significance can be determined due to the large uncertainties on their compositions. One of the most intriguing aspects of the hibonite grains is that they have both large positive and large negative anomalies in, for example, $\varepsilon^{50}\mathrm{Ti}_{(47/49)}$ (see Figure 1). The two remaining components represent the sources of hibonite grains that exhibit negative anomalies in $\varepsilon^{50}\mathrm{Ti}_{(47/49)}$ and $\varepsilon^{46}\mathrm{Ti}_{(47/49)}$. These large positive and negative anomalies are difficult to reconcile with the very small range in bulk meteorites in the context of binary mixing. However, in the context of binary mixing between multiple sources, these anomalies are more easily understood. Broadly, component {2} constitutes negative $\gamma(^{50}\mathrm{Ti}_{(47/49)})$, negative $\gamma(^{46}\mathrm{Ti}_{(47/49)})$, and positive $\gamma(^{48}\mathrm{Ti}_{(47/49)})$, while component {3} is made up of negative $\gamma(^{50}\mathrm{Ti}_{(47/49)})$, positive $\gamma(^{46}\mathrm{Ti}_{(47/49)})$, and negative $\gamma(^{48}\mathrm{Ti}_{(47/49)})$. These two components are not well defined enough to quantitatively discuss the nucleosynthetic significance; however, qualitative assessments may be made. Component {2} is consistent with input from material from low-mass ($\sim$13–15 $M_{\odot}$) SN II models, while the sources of component {3} are consistent with several mid-mass ($\sim$25–30 $M_{\odot}$) SN II (Hashimoto 1995; Umeda & Nomoto 2002). Even though the sources cannot be definitively identified, these components are still useful for discussing potential mixing environments within the solar system as they are helpful for interpreting the hibonite data (see Section 4.3).

4.3. Implications for Mixing and Sources within the Solar System

The ICA of the hibonite data returns the compositions of three components that most likely reflect mixing of four sources. Most of the data cluster around zero, which suggests that one of the sources is represented by this composition. Interestingly, this composition is compatible with the composition of one of the bulk meteorite sources. This may be close in composition to one of the ends of the bulk meteorite correlation and could represent the bulk composition of the presolar molecular cloud (see Section 4.3.1). That one of the sources of the two different sample sets may be the same is interesting and also may present a more likely scenario because it reduces the number of required sources. However, we must examine the likelihood that such a source may exist.

4.3.1. Material in Proto-planetary Disks, Molecular Clouds, and the Interstellar Medium

The identity of the material of this shared composition is likely the average of highly processed material from the parent molecular cloud. The journey of stellar condensates from stars and supernovae to proto-planetary disks is not a simple one. There are many stages of processing and mechanisms by which they may be altered and destroyed.

The solar system, and proto-planetary disks in general, form from a mixture of material from many different generations of stars likely integrating material over billions of years of galactic evolution. Indeed, it has been estimated that the timescale for a grain from a stellar sources to traverse the interstellar medium (ISM) and be incorporated into a proto-planetary disk is on the order of a 1 Ga (Dwek & Scalo 1980; Jones & Nuth 2011). However, due to physical processing and irradiation in the

ISM it is an oversimplification to assume that the material in a molecular cloud contains the original isotopic signatures of stars integrated over 1 or 2 Ga.

Material in molecular clouds may have experienced several cycles through the diffuse ISM into molecular clouds without necessarily being incorporated into a proto-planetary disk, or a star, to be reprocessed. Lifetimes of refractory grains have been estimated at 4×10^8–20×10^8 yr, depending on how much time the grains spend in molecular clouds where stars are more likely to form (see Barlow 1978; Jones 2004 for discussions). Interestingly, Molster & Waters (2003) note that crystalline silicates are only observed around supernovae and young stars and proto-planetary disks—where they are likely to be forming. This suggests from an observational standpoint that fresh material does not last long in the ISM. Carrez et al. (2002) performed laboratory experiments to investigate the effects of He irradiation of olivine as an analog to radiation processing in ISM, finding that both chemical and structural changes occur in olivine culminating in amorphization. While, from astronomical observations, Kemper et al. (2004) find that the timescale of amorphization in the ISM is on the order of 5–9 Ma.

Therefore, in most cases, the lifetime of grains will be less than the timescale from production in supernova to processing in proto-planetary disk. It follows, then, that many grains will not survive their journey through the ISM to be incorporated into a proto-planetary disk. Rather these grains will become amorphized and eventually destroyed. This material will remain in the ISM and form new grains. Jones & Nuth (2011) estimate that the majority (90%–95%) of grains observed in the ISM would have formed in situ and so will not represent pure stellar compositions. The action of this grain reformation will be to homogenize the isotopic compositions of the many generations and types of stars that have given material to the ISM. From this argument alone it seems logical that material from the majority of old stellar sources will have been homogenized to yield a single, averaged composition in the early solar system and not a multitude of grains with highly exotic compositions integrating stellar sources over billions of years. Moreover, as Molster & Waters (2003) describe, crystalline grains are only observed around young stars (proto-planetary disks) and evolved stars (e.g., winds from an AGB) but not in the ISM. This suggests that the grains that are forming in the ISM are amorphous and may be more volatile and so may have been more easily further homogenized by higher-temperature processing in the proto-solar nebula.

Younger grains from more recent events ($\ll$1 Ga to $\sim$1 Ma prior to the formation of the proto-solar nebula), however, are more likely to survive intact and to remain crystalline. Therefore, more recent events may still present grains with large anomalies to the early solar system. Due to the lifetime of grains (5–20×10^8 yr; Barlow 1978) it is unlikely they will have been destroyed to form new phases so will not reflect the homogenized isotopic compositions of the host molecular cloud or ISM. However, to a variable degree, they will likely have experienced processing in the ISM or molecular cloud, and this may affect their ability to contribute to isotopic heterogeneity in the proto-planetary disk.

An important point to clarify here is what the anomalies that are measured mean in terms of grains or carrier phases. To present an isotopic anomaly in the early solar system, grains must be heterogeneously distributed. For example, large anomalies are present in CC leachates in Zr isotopes (Schönbächler et al. 2005); however, much smaller anomalies are present in the bulk meteorites (Akram et al. 2013). This is because the carrier phase of Zr isotopes anomalies was relatively homogeneously distributed between the different chondrite parent bodies. For the bulk meteorites, normal CAI and hibonite populations of interest to this study, the anomalies represent different abundances of carrier phases. Therefore, the effectiveness of a grain to transfer an anomaly from a stellar source to a proto-planetary disk relies on its ability to either remain, or become, heterogeneously distributed through the nebula. Factors that may affect this are volatility, as volatile grains are effectively mixed as they enter the gas phase; crystallinity, as more crystalline phases may be more refractory but also effectively sorted by physical processes such as photophoresis (Krauss & Wurm 2005; Wurm et al. 2010); size; density; or chemistry. Clearly some of the factors are more important than others; if the grains are chemically unstable or volatile, size and density sorting will be less significant. Therefore, we can examine the effects of processing in the molecular cloud and ISM on some of these important factors for the preservation of anomalies.

4.3.2. Relationships between Hibonite and Bulk Meteorite Sources

We find that the sources of the hibonite Ti isotope anomalies are not related to the sources of the bulk meteorite anomalies (see Section 3.1). This is an interesting finding because while the hibonites represent the largest Ti isotope anomalies in the solar system, the bulk meteorites constitute much more material and so actually contain a much greater mass of anomalous Ti. Therefore, it might have been expected that these two repositories of anomalous Ti share a common source.

There are two end-member explanations for why the hibonite sources and the bulk meteorites sources are not the same.

1. The dominant source in the bulk meteorites is not a primary nucleosynthetic source(s) as previously thought (e.g., Leya et al. 2008, 2009; Qin et al. 2011; Steele et al. 2012) but rather is made within the solar system by mixing one or more of the hibonite sources, or some other sources, at some point after hibonite formation but before CAI formation as normal CAIs sample the same sources as the bulk meteorites (Trinquier et al. 2009).
2. The hibonite sources, while highly concentrated in the hibonite forming regions, are not dominant in the solar system and have been diluted to extinction during subsequent mixing.

The first scenario poses the very interesting prospect of being able to directly examine the timescales of early solar system mixing in the early solar system. By dating hibonite formation we may find the final time at which primary nucleosynthetic sources were sampled. This may then be compared with the age of CAI formation, after which time full solar system mixing of the primary sources had occurred. This comparison would yield information about the time taken for large-scale homogenization of the primary nucleosynthetic sources. As discussed above, and in previous studies (e.g., Ireland 1990), the hibonites with the largest anomalies are the PLACs; these then might represent the earliest samples. The SHIBs have much smaller, or no, stable isotope anomalies coupled with variable ^{26}Al abundances (Sahijpal & Goswami 1998). The SHIBs may simply represent hibonite formation contemporaneously with the PLACs, but in a region with lower abundances of anomalous Ti carriers and higher abundances of ^{26}Al carriers

(Liu et al. 2012). Alternatively, the SHIBs may represent an intermediate stage of mixing between the PLAC sources and the bulk meteorite sources, possibly the carrier phase for the bulk meteorite variation.

While it is certainly a possibility that the SHIBs represent an intermediate stage of mixing, the current level of precision on Ti isotope compositions of the hibonite population are not high enough to determine if this is the case. However, we can place limits on the extent of mixing that would have had to occur. The precision of the hibonite measurements would place the bulk meteorite source composition only +200 $^{0}/_{000}$ in $\varepsilon^{50}\mathrm{Ti}_{(47/49)}$ and +40 $^{0}/_{000}$ in $\varepsilon^{46}\mathrm{Ti}_{(47/49)}$. In order to create the variation in $\varepsilon^{50}\mathrm{Ti}_{(47/49)}$ from SHIBs with this composition would require hibonite abundances between 50 and 200 times those observed in CM hibonites, depending on Ti concentration in the hibonites (using concentration and abundance data from Ireland et al. 1988 and Wasson & Kallemeyn 1988). Under nebula conditions, outside the CAI forming region, hibonite is a physically, chemically, and thermally stable mineral; therefore, if hibonite grains had been present in these abundances, it seems unlikely it would been depleted so significantly in all chondrite groups, especially in primitive groups such as CM chondrites. Moreover, other chondrites contain even lower abundances of hibonite, so would require even more complete reprocessing. Therefore, we favor the second model in which the hibonite sources, although highly anomalous in the hibonite forming region, are not dominant on a bulk solar system scale (e.g., Boss 2008).

The second scenario, in which the sources of hibonite Ti isotope anomalies are diluted to extinction during the final stages of homogenization in the protosolar nebula, makes the hibonite source compositions less significant for the bulk composition of the solar system. However, these sources record nucleosynthetic information not present in other early solar system samples and so may provide a tantalizing, fine scale view of the astrophysical birth environment of the solar system. They may record the compositions of stellar environments that, while not dominant, contributed material to the solar system while it was forming. In this way, they may provide a more complete view of all of the stellar sources to the proto-solar nebula.

The sources of hibonite Ti isotope anomalies were not homogenized into the molecular cloud composition; therefore they must be younger than around 100 Ma (see Section 4.3.1). These sources were likely some combination of SN Ia and SN II. The grains in material ejected during these events would still be crystalline after ~100 Ma and so would have remained relatively impervious to thermal processing during the early collapse of the proto-solar nebula. This relatively recently synthesized material may have been concentrated in clumps as it has not had as much time to be processed and mixed into the molecular cloud, so could survive in relatively concentrated clumps in the proto-solar nebula. These clumps may be distributed throughout the proto-solar nebula, but the only samples we derive from this time were in the hibonite forming region. It is in these clumps that the hibonites would form, partially mixing with homogenized molecular cloud material to give the compositions we observe in the hibonites today. Subsequently, these clumps would be dynamically mixed into the rest of the solar system (e.g., Boss 2008; Ciesla 2009).

There are three mechanisms by which the highly anomalous material in these clump would not dominate the bulk meteorite compositions that formed later. First, the sources may have been in such low concentration in the bulk proto-solar nebula that they were simply be diluted to extinction. Second, they may have been somewhat amorphized by radiation damage in the molecular cloud and more susceptible to the thermal processing than the bulk meteorite source. Last, the majority of the material may have been lost to the proto-Sun during infall and that the hibonite grains were propelled back out into the solar system on stellar winds or in bipolar outflow jets (e.g., Shu et al. 2001).

In addition to large stable isotope anomalies, the PLACs, which best represent the hibonite sources, are devoid of evidence for live ^{26}Al. Therefore, the hibonites may have formed from material devoid of ^{26}Al, either dominantly from a supernova zone that does not produce ^{26}Al or from material older than $\gtrsim$5 Ma. A second possibility is that the hibonite grains formed contemporaneously with CAIs and experienced a thermal event in the solar system ~5 Ma after CAI formation, which would have erased any signature of ^{26}Al. However, if the hibonite and normal population of CAIs formed contemporaneously, it is difficult understand why the hibonite grains have such large stable isotope anomalies.

4.3.3. Why Is the Bulk Meteorite Source Dominant?

There is evidence that a wide variety of different nucleosynthetic sources were present in the proto-solar nebula. However, only one of these sources dominates the Ti isotope variation in the bulk meteorites. Taking again the example of Ti, the O/Ne zone from an SN II appears to be the dominant source in the bulk meteorites, and so the bulk solar system. It is possible that this source is dominant simply because it is the most concentrated. However, due to processing in the ISM, material from older stellar sources may be more readily homogenized in the early solar system (see Section 4.3.1). In this way, material from more recent nucleosynthetic sources may be more resistant to mixing in the early solar system. Therefore, the dominant sources in the bulk meteorites and normal CAIs may not be the most concentrated but the freshest, or more recently synthesized. With further studies, it may be possible to test this hypothesis by examining potential correlations between the sources of stable isotope anomalies (like Ti) and the sources of SLRs (like ^{26}Al).

5. CONCLUSIONS

We have examined mixing relationships in the early solar system by comparing the sources of Ti isotope variation. Using ICA we have compared the sources of Ti isotope variation in hibonite grains and bulk meteorites. We find the variation in bulk meteorites represents mixing of three sources, while the hibonite populations are consistent with mixing of four sources. The ICA shows that the highly anomalous sources of bulk meteorite and hibonite Ti isotope variation are not related. One source is hypothesized, which is consistent between both data sets and has a composition close to the terrestrial ratio. This source may be represented by molecular cloud material, highly processed, and homogenized by radiation and thermal events significantly before the start of the solar system.

The finding that the anomalous nucleosynthetic sources represented by the variation in hibonite and bulk meteorites are not related has significant implications for mixing in the early solar system. One possible explanation is that the sources that dominate the variation in the bulk meteorites are not primary nucleosynthetic sources but rather were created by mixing two or more hibonite sources. However, this requires a stage of full proto-solar nebula mixing from which we derive no samples. An alternative hypothesis is that the hibonite sources, although dominant in the hibonite forming regions, are not significant

sources for isotope anomalies in the bulk solar system. This may be because the sources were of low concentration after major homogenization had occurred. Another, possibly more likely, hypothesis is that is that the carrier phases of the hibonite Ti isotope anomalies, while abundant, were not physically or chemically robust enough to survive the vigorous mixing in the proto-solar nebula.

We thank Kevin McKeegan and Ming-Chang Liu for detailed and insightful comments, thorough discussion, and encouragement. We also thank Andrew Davis and Levke Kööp for reviewing this manuscript and their detailed comments that greatly improved the manuscript. We thank Eric Feigelson for his editorial handling. We are grateful for funding for this work from UCLA and NASA Cosmochemistry (grant NNX13AD13G).

APPENDIX

Mass-independent Ti isotope anomalies in hibonites and meteorites have been presented using a variety of normalizing ratios including $^{46}Ti/^{48}Ti$ and $^{47}Ti/^{49}Ti$ (see Section 2.3 in the main text). In order for these data to be comparable, they must be renormalized to the same ratio. Trinquier et al. (2009) recently reported Ti isotope variations in bulk meteorites and found that the variations are most easily explained by correlated anomalies on the isotopes ^{46}Ti and ^{50}Ti, thus the $^{47}Ti/^{49}Ti$ normalization provides the most precise correction that does not include clear anomalies. Therefore, we have renormalized previous hibonite data to the $^{47}Ti/^{49}Ti$ ratio (see Table A1 and Section 2.1 in the main text for more details).

Table A1
Table of Renormalized Hibonite Ti Isotope Compositions

Sample Name	Type	Reference	$\varepsilon^{46}Ti_{(47/49)}$	2 s.d.	$\varepsilon^{48}Ti_{(47/49)}$	2 s.d.	$\varepsilon^{50}Ti_{(47/49)}$	2 s.d.
7-76	SHIB	Ireland 1990	−6.1	64.6	2.0	29.8	36.9	87.1
7-143	SHIB	Ireland 1990	8.1	8.7	2.0	4.7	28.1	14.5
7-290	SHIB	Ireland 1990	39.6	68.8	6.9	31.1	−57.4	91.5
7-373	SHIB	Ireland 1990	−9.8	64.9	7.6	27.7	−4.8	79.2
7-412	PLAC	Ireland 1990	5.4	7.1	14.6	4.1	40.4	14.0
7-505	SHIB	Ireland 1990	−4.3	44.3	12.1	19.6	25.8	57.8
7-551	SHIB	Ireland 1990	−1.1	59.7	3.0	26.9	33.0	83.7
7-644	PLAC	Ireland 1990	69.5	80.5	31.5	33.8	−13.0	93.3
7-658	PLAC	Ireland 1990	58.0	63.9	46.7	28.7	55.9	84.4
7-664	SHIB	Ireland 1990	6.3	8.9	21.6	5.2	22.3	17.5
7-734	SHIB	Ireland 1990	11.9	49.7	20.1	22.0	25.9	63.4
7-789	SHIB	Ireland 1990	5.8	5.5	16.1	3.3	11.9	12.7
7-821	SHIB	Ireland 1990	20.9	51.4	−0.6	23.3	58.7	69.1
7-953	SHIB	Ireland 1990	9.4	9.0	16.6	5.2	16.4	18.0
7-980	PLAC	Ireland 1990	−10.1	10.7	23.7	6.4	−110.0	18.1
7-981	PLAC	Ireland 1990	−16.1	7.1	19.7	4.1	−112.0	12.8
7-A84	SHIB	Ireland 1990	−8.1	38.9	−2.0	18.0	24.9	52.9
7-A95	SHIB	Ireland 1990	30.2	59.9	−9.6	24.8	−53.7	69.6
8-47	SHIB	Ireland 1990	12.6	40.8	7.5	18.7	7.6	53.4
8-49	SHIB	Ireland 1990	50.9	64.2	7.9	29.0	−34.3	77.8
8-65	SHIB	Ireland 1990	5.1	44.7	−1.0	19.5	19.1	59.0
8-66	PLAC	Ireland 1990	−24.3	66.6	23.8	27.9	−208.0	80.3
13-02	SHIB	Ireland 1990	−11.0	45.0	−9.0	20.6	28.9	69.1
13-03	SHIB	Ireland 1990	4.2	29.4	−6.0	14.2	20.1	43.3
13-04	SHIB	Ireland 1990	−16.5	31.2	12.1	14.9	29.6	45.0
13-13	PLAC	Ireland 1990	119.0	59.7	−38.2	24.0	2491.0	68.9
13-23	BAG	Ireland 1990	−40.2	45.8	5.7	19.1	−178.0	50.6
13-24	SHIB	Ireland 1990	−33.0	69.0	2.7	31.4	146.0	93.5
13-25	PLAC	Ireland 1990	64.8	64.6	40.1	29.3	−350.0	85.9
13-33	SHIB	Ireland 1990	−69.5	55.5	−40.2	25.8	0.0	80.6
13-37	SHIB	Ireland 1990	−10.5	43.4	−9.5	19.5	13.5	54.0
13-51	PLAC	Ireland 1990	40.5	82.6	47.8	36.5	−379.0	104.0
13-60	SHIB	Ireland 1990	−6.6	37.2	−3.5	16.7	−24.5	46.3
13-61	SHIB	Ireland 1990	23.7	39.6	−17.1	17.3	−5.4	48.5
14-12	PLAC	Ireland 1990	−46.1	48.9	−0.3	22.3	−210.0	63.5
14-14	SHIB	Ireland 1990	−4.1	33.6	2.0	14.8	44.9	43.1
Mur-A1	...	Zinner et al. 1986	−61.9	27.3	−18.3	11.6	70.9	32.1
Mur-H7	...	Zinner et al. 1986	15.5	12.6	−15.1	9.1	58.2	31.4
Mur-H8	...	Zinner et al. 1986	−7.9	41.0	−14.0	16.8	−1.9	48.7
Mur-20	...	Zinner et al. 1986	4.7	7.0	23.1	4.1	−433.0	13.9
Mur-70	...	Zinner et al. 1986	−10.7	6.5	30.3	4.8	−222.0	15.6
Mur-170	...	Zinner et al. 1986	33.2	6.8	−6.6	3.6	−539.0	12.0
My-H3	...	Zinner et al. 1986	48.1	25.8	−11.2	11.7	955.0	35.5
My-H4	...	Zinner et al. 1986	47.0	58.5	−10.2	23.6	971.0	65.0
CH-B2	PLAC	Sahijpal et al. 2000	−4.8	39.4	−17.0	18.4	502.0	65.1
CH-B7	PLAC	Sahijpal et al. 2000	99.8	43.2	−11.8	21.4	121.0	79.9

Table A1
(Continued)

Sample Name	Type	Reference	$\varepsilon^{46}Ti_{(47/49)}$	2 s.d.	$\varepsilon^{48}Ti_{(47/49)}$	2 s.d.	$\varepsilon^{50}Ti_{(47/49)}$	2 s.d.
CH-A5	SHIB	Sahijpal et al. 2000	11.1	38.3	−28.6	16.3	−15.8	47.9
CH-B5	PLAC	Sahijpal et al. 2000	21.7	37.6	−25.1	22.3	138.0	65.1
All-3529-42	...	Sahijpal et al. 2000	13.6	53.4	10.5	25.1	22.6	72.1
CH-A3	SHIB	Sahijpal et al. 2000	−11.3	73.8	−22.5	35.9	86.4	109.0
CH-B3	PLAC	Sahijpal et al. 2000	7.8	46.5	−11.6	22.0	92.5	75.7
CH-A4	SHIB	Sahijpal et al. 2000	2.1	71.2	−35.5	34.9	577.0	115.0
Mur-S15	SHIB	Liu et al. 2009	−96.9	71.9	−27.1	35.2	15.3	110.0
Mur-P1	PLAC	Liu et al. 2009	23.5	78.8	−3.1	41.8	496.0	133.0
Mur-P2	PLAC	Liu et al. 2009	−50.1	85.7	−29.8	41.8	232.0	133.0
Mur-P6	PLAC	Liu et al. 2009	−113.0	79.0	38.1	37.4	−39.8	117.0
Mur-P7	PLAC	Liu et al. 2009	−140.0	75.4	−35.8	38.0	2058.0	116.0
Mur-P8	PLAC	Liu et al. 2009	−181.0	79.4	5.2	38.2	38.6	119.0
Mur-P9-spot1	PLAC	Liu et al. 2009	−273.0	94.8	30.5	44.4	−335.0	130.0
Mur-P9-spot2	PLAC	Liu et al. 2009	−245.0	74.4	53.1	35.9	−410.0	107.0
Mur-B1-spot1	BAG	Liu et al. 2009	123.0	105.0	37.4	47.6	−50.2	139.0
Mur-B1-spot1-1	BAG	Liu et al. 2009	138.0	117.0	44.9	51.4	−143.0	140.0
Mur-B1-spot2	BAG	Liu et al. 2009	54.1	108.0	34.5	53.3	−449.0	159.0
Mur-B1-spot2-1	BAG	Liu et al. 2009	−72.6	122.0	9.9	54.4	−247.0	145.0
Mur-B1-spot3	BAG	Liu et al. 2009	−35.3	85.9	−10.9	39.9	−113.0	110.0
Mur-B1-spot3-1	BAG	Liu et al. 2009	−0.9	94.1	48.5	44.4	−16.0	126.0
MUR-Al-a	...	Fahey et al. 1985	7.1	65.9	1.0	26.2	82.1	73.7
MUR-Al-b	...	Fahey et al. 1985	−9.6	29.0	−0.5	12.8	48.4	35.7
MUR-H7	...	Fahey et al. 1985	15.5	25.2	−15.1	10.3	58.2	27.7
MY-H3-a	...	Fahey et al. 1985	32.7	29.0	−10.1	13.0	971.0	41.5
MY-H3-b	...	Fahey et al. 1985	103.0	56.3	−12.8	24.7	902.0	68.1
ATP-1	...	Fahey et al. 1985	−25.4	23.8	1.1	10.2	10.6	29.8
ATP-2-a	...	Fahey et al. 1985	−27.5	36.9	3.1	16.3	−1.5	52.1
ATP-2-b	...	Fahey et al. 1985	−0.3	46.9	16.1	18.3	17.8	49.3
ATP-3-a	...	Fahey et al. 1985	15.4	35.1	−7.1	15.5	21.3	44.6
ATP-3-b	...	Fahey et al. 1985	35.5	32.1	8.9	14.6	25.3	42.5
C-1	FUN	Niederer 1980	−10.6	1.6	0.6	0.7	−39.0	1.8
C-2	FUN	Niederer 1980	−11.8	1.8	1.2	0.8	−37.9	2.8
EK-1-4-1	FUN	Niederer 1980	−13.2	4.4	−15.5	2.5	17.6	9.7
EK-1-4-2	FUN	Niederer 1980	−9.8	3.4	−14.3	1.7	16.1	4.8
EK-1-4-3	FUN	Niederer 1980	−7.7	11.3	−18.0	6.4	15.1	19.3
EK-1-4-4	FUN	Niederer 1980	−6.1	5.6	−16.4	2.6	10.0	7.3
EK-1-4-5	FUN	Niederer 1980	−8.8	4.8	−16.3	2.1	14.8	5.4
DJ-1	...	Hinton et al. 1987	−2.7	22.3	6.5	15.2	−190.0	58.9
BB-5	...	Hinton et al. 1987	−7.1	23.8	52.6	16.3	−578.0	56.9
BB-5-c	...	Hinton et al. 1987	−0.6	26.7	58.1	10.3	−573.0	25.6
Gr-1-r	...	Hinton et al. 1987	39.1	23.5	7.4	12.3	−93.8	53.8
Gr-1-c	...	Hinton et al. 1987	34.3	37.9	−9.7	16.0	−105.0	44.7
SH-7	...	Hinton et al. 1987	1.6	20.3	−3.5	7.7	160.0	17.3
Mur-H9	...	Fahey et al. 1987a	−26.8	32.0	−7.4	14.1	147.0	42.8
My-CH1	...	Fahey et al. 1987a	−2.0	23.4	−4.0	10.2	30.0	29.5
MY-IP	...	Fahey et al. 1987a	5.0	47.3	3.0	19.8	−1.0	56.0
CB-H2	...	Fahey et al. 1987a	−1.1	24.2	5.0	10.9	−3.1	36.1
CB-H4	...	Fahey et al. 1987a	17.4	35.3	−5.1	16.0	133.0	48.2
HAL-Ha	...	Fahey et al. 1987a	13.4	71.0	18.6	30.4	188.0	87.0
HAL-Hb	...	Fahey et al. 1987a	30.0	52.1	6.4	23.9	124.0	73.3
DA2-12	...	Fahey et al. 1987a	32.3	35.0	−15.6	15.5	49.9	45.0
ATP-1b	...	Fahey et al. 1987a	5.5	20.5	4.5	8.5	23.5	23.8
MUR-H1	Hib	Fahey et al. 1987b	17.7	23.7	−29.1	10.3	65.2	30.3
BB-5-H	Hib	Fahey et al. 1987b	−34.7	27.6	59.9	12.8	−574.0	37.4
BB-5-C	Corr	Fahey et al. 1987b	−20.8	46.8	50.1	20.7	−581.0	58.4

Notes. Table showing Ti isotope compositions of hibonites from literature. The data have been renormalized from the $^{46}Ti/^{48}Ti$ normalization to the $^{47}Ti/^{49}Ti$ normalization used by more recent bulk meteorite studies. Uncertainties were estimated using a Monte Carlo simulation as described in the text.

REFERENCES

Akram, W., Schönbächler, M., Sprung, P., & Vogel, N. 2013, ApJ, 777, 169
Barlow, M. J. 1978, MNRAS, 183, 367
Boss, A. P. 2008, E&PSL, 268, 102
Burkhardt, C., Kleine, T., Oberli, F., et al. 2011, E&PSL, 312, 390
Carrez, P., Demyk, K., Cordier, P., et al. 2002, M&PS, 37, 1599
Ciesla, F. J. 2009, Icar, 200, 655
Comon, P. 1994, SigPr, 36, 287
Cuesta-Albertos, J., Gordaliza, A., Matrán, C., et al. 1997, AnSta, 25, 553

Dauphas, N., Cook, D. L., Sacarabany, A., et al. 2008, ApJ, 686, 560
Dauphas, N., Davis, A., Marty, B., & Reisberg, L. 2004, E&PSL, 226, 465
Dauphas, N., Remusat, L., Chen, J. H., et al. 2010, ApJ, 720, 1577
Dwek, E., & Scalo, J. M. 1980, ApJ, 239, 193
Efron, B. 1981, Biometrika, 68, 589
Fahey, A., Goswami, J. N., McKeegan, K. D., & Zinner, E. 1985, ApJL, 296, L17
Fahey, A. J., Goswami, J. N., McKeegan, K. D., & Zinner, E. K. 1987a, GeCoA, 51, 329
Fahey, A. J., Goswami, J. N., McKeegan, K. D., & Zinner, E. K. 1987b, ApJL, 323, L91
Fritz, H., Garcıa-Escudero, L. A., & Mayo-Iscar, A. 2012, J. Stat. Softw., 47, 12
Hashimoto, M. 1995, PThPh, 94, 663
Heydegger, H. R., Foster, J. J., & Compston, W. 1979, Natur, 278, 704
Hinton, R. W., Davis, A. M., & Scatena-Wachel, D. E. 1987, ApJ, 313, 420
Hyvarinen, A. 1999, ITNN, 10, 626
Hyvärinen, A., & Oja, E. 2000, NN, 13, 411
Ireland, T. R. 1990, GeCoA, 54, 3219
Ireland, T. R., Fahey, A. J., & Zinner, E. K. 1988, GeCoA, 52, 2841
Ireland, T. R., Zinner, E. K., Fahey, A. J., & Esat, T. M. 1992, GeCoA, 56, 2503
Iwamori, H., & Albarède, F. 2008, GGG, 9, 1
Iwamoto, K., Brachwitz, F., Nomoto, K., et al. 1999, ApJS , 125, 439
Jones, A. P. 2004, in ASP Conf. Ser. 309, Astrophysics of Dust, ed. A. N. Witt, G. C. Clayton, & B. T. Draine (San Francisco, CA: ASP), 347
Jones, A. P., & Nuth, J. A. 2011, A&A, 530, A44
Kemper, F., Vriend, W. J., & Tielens, A. G. G. M. 2004, ApJ, 609, 826
Krauss, O., & Wurm, G. 2005, ApJ, 630, 1088
Lee, T., Papanastassiou, D. A., & Wasserburg, G. J. 1978, ApJL, 220, L21
Leya, I., Schönbächler, M., Krähenbühl, U., & Halliday, A. N. 2009, ApJ, 702, 1118
Leya, I., Schönbächler, M., Wiechert, U., Krähenbühl, U., & Halliday, A. N. 2008, E&PSL, 266, 233
Liu, M.-C., Chaussidon, M., Göpel, C., & Lee, T. 2012, E&PSL, 327, 75
Liu, M.-C., McKeegan, K. D., Goswami, J. N., et al. 2009, GeCoA, 73, 5051
Lyons, J., & Young, E. 2005, Natur, 435, 317
Lyons, J. R., Bergin, E. A., Ciesla, F. J., et al. 2009, GeCoA, 73, 4998
Maeda, K., Röpke, F. K., Fink, M., et al. 2010, ApJ, 712, 624
Mahon, K. 1996, Int. Geol. Rev., 38, 293
Marchini, J., Heaton, C., & Ripley, B. 2013, Fastica: Fastica Algorithms to Perform ICA and Projection Pursuit, R Package Version 1 (Oxford: Univ. Oxford), http://cran.r-project.org/web/packages/fastICA/index.html
Marhas, K. K., Goswami, J. N., & Davis, A. M. 2002, Sci, 298, 2182
McCulloch, M. T., & Wasserburg, G. J. 1978, ApJL, 220, L15
Meyer, B. S., Krishnan, T. D., & Clayton, D. D. 1996, ApJ, 462, 825
Meyer, B. S., Weaver, T. A., & Woosley, S. E. 1995, Metic, 30, 325
Molster, F., & Waters, L. 2003, in Astromineralogy, ed. T. Henning (Lecture Notes in Physics, Vol. 609; Berlin: Springer), 121
Niederer, F. R., Papanastassiou, D. A., & Wasserburg, G. J. 1980, ApJL, 240, L73
Niederer, F. R., Papanastassiou, D. A., & Wasserburg, G. J. 1985, GeCoA, 49, 835
Niemeyer, S., & Lugmair, G. W. 1980, Metic, 15, 341
Niemeyer, S., & Lugmair, G. W. 1981, E&PSL, 53, 211
Nomoto, K., Hashimoto, M., Tsujimoto, T., et al. 1997, NuPhA, 616, 79
Qin, L., Nittler, L. R., Alexander, C. M. O., et al. 2011, GeCoA, 75, 629
Rauscher, T., Heger, A., Hoffman, R. D., & Woosley, S. E. 2002, ApJ, 576, 323
R Core Team 2013, R: A Language and Environment for Statistical Computing (Vienna: R Foundation for Statistical Computing), http://www.R-project.org/
Russell, W., Papanastassiou, D., & Tombrello, T. 1978, GeCoA, 42, 1075
Sahijpal, S., & Goswami, J. N. 1998, ApJL, 509, L137
Sahijpal, S., Goswami, J. N., & Davis, A. M. 2000, GeCoA, 64, 1989
Schönbächler, M., Rehkämper, M., Fehr, M. A., et al. 2005, GeCoA, 69, 5113
Shu, F., Shang, H., Gounelle, M., Glassgold, A., & Lee, T. 2001, ApJ, 548, 1029
Steele, R. C. J., Coath, C. D., Regelous, M., Russell, S., & Elliott, T. 2012, ApJ, 758, 59
Steele, R. C. J., Elliott, T., Coath, C. D., & Regelous, M. 2011, GeCoA, 75, 7906
Thiemens, M. H. 1999, Sci, 283, 341
Travaglio, C., Hillebrandt, W., Reinecke, M., & Thielemann, F. 2004, A&A, 425, 1029
Travaglio, C., Röpke, F. K., Gallino, R., & Hillebrandt, W. 2011, ApJ, 739, 93
Trinquier, A., Birck, J. L., Allègre, C. J., Göpel, C., & Ulfbeck, D. 2008, GeCoA, 72, 5146
Trinquier, A., Elliott, T., Ulfbeck, D., et al. 2009, Sci, 324, 374
Umeda, H., & Nomoto, K. 2002, ApJ, 565, 385
Usui, T., & Iwamori, H. 2013, M&PS, 48, 2289
Völkening, J., & Papanastassiou, D. A. 1989, ApJL, 347, L43
Wasson, J. T., & Kallemeyn, G. W. 1988, RSPTA, 325, 535
Williams, N., Schönbächler, M., Fehr, M., Akram, A., & Parkinson, I. 2014, LPSC, 45, 2183
Woosley, S. E. 1997, ApJ, 476, 801
Wurm, G., Teiser, J., Bischoff, A., Haack, H., & Roszjar, J. 2010, Icar, 208, 482
York, D. 1969, E&PSL, 5, 320
Young, E. D., Galy, A., & Nagahara, H. 2002, GeCoA, 66, 1095
Zhang, J., Dauphas, N., Davis, A. M., Leya, I., & Fedkin, A. 2012, NatGe, 5, 251
Zhang, J., Dauphas, N., Davis, A. M., & Pourmand, A. 2011, J. Anal. At. Spectrom., 26, 2197
Zinner, E. 2003, in Treatise on Geochemistry, Vol. 1, ed. H. D. Holland & K. K. Turekian (Oxford: Elsevier-Pergamon), 17
Zinner, E., Jadhav, M., Gyngard, F., & Nittler, L. 2010, M&PSA, 73, 5137
Zinner, E. K., Fahey, A. J., McKeegan, K. D., Goswami, J. N., & Ireland, T. R. 1986, ApJL, 311, L103